Comparative analysis of offshore support structures for two-bladed large wind turbines (10+MW) in deep waters

Vergassola, Marco; Cabboi, Alessandro; van der Male, Pim

DOI
10.1088/1742-6596/1618/5/052076

Publication date
2020

Document Version
Final published version

Published in
Journal of Physics: Conference Series

Comparative analysis of offshore support structures for two-bladed large wind turbines (10+MW) in deep waters

Comparative analysis of offshore support structures for two-bladed large wind turbines (10+MW) in deep waters

Marco Vergassola*, Alessandro Cabboi and Pim van der Male

Faculty of Civil Engineering and Geosciences, Delft University of Technology, Stevinweg 1, 2628CN Delft, NL

E-mail: *M.Vergassola@tudelft.nl

Abstract.

The offshore wind market is developing towards exploiting wind resources in deeper water sites. Inevitably, this fuels new research and feasibility studies on alternative solutions for the wind turbine support structures. Within this context, this work aims at comparing three different support structure design concepts for a 14 MW two-bladed downwind wind turbine: an XXL monopile, a hybrid jacket-tower and a lattice tower. To ensure a fair comparability of the three design concepts, a load capacity analysis is first performed to assess the yield strength of each concept and guarantee a similar material utilization. The comparative analysis is then carried out in terms of total mass, dynamic behaviour of the interaction between rotor and support structure, soil-structure interaction and resulting hydrodynamic forces. Based on the given design constraints, the preliminary results of this study favour a lattice tower solution. The study also highlights peculiar dynamic phenomena such as veering, mode hybridization and mode coalescence for the dynamic interaction between the lattice tower and the two-bladed rotor which need to be taken into account during the design phase.

1. Introduction

The increasing size of wind turbines and the need to start exploiting wind resources in deeper water sites are introducing new challenges for the offshore wind industry. Researchers are now focused on the study of the so-called XXL monopile support structures which introduce significant problems in terms of manufacturing, installation and sensitiveness towards soil-structure interaction [1, 2]. An alternative solution is represented by the hybrid jacket-tower concept, consisting of a space-frame substructure supporting a tubular tower. A first advantage of a space-frame structure relies on the slenderness of its foundation piles, whose corresponding soil-structure interaction is relatively easier to handle compared to the soil-monopile interaction [3]. A recent study [4], which aimed at comparing the estimated mass for a jacket-tower and for a monopile-tower concept, showed that the monopile concept seems to be preferable to jackets up to water depths of approximately 40 m. However, the jacket concept still requires an expensive transition piece [5] and does not fully exploit the potential of a space-frame structure. The aforementioned result can be challenged by considering a full-height lattice concept which provides a larger margin of optimizing its configuration in order to achieve an even larger weight reduction [6, 7].

Within this framework, the objective of this study is to compare three different support structure concepts: a) the monopile-tower configuration; b) the hybrid jacket-tower concept; c) the lattice structure. The primary target of the comparative study was to provide an order of magnitude of the possible mass reduction that can be achieved by adopting a space-frame concept. However, the gain in mass reduction comes with a cost that is reflected by a more complex dynamic behaviour caused by the interaction between the space-frame supporting structure and the rotor-nacelle-assembly.

All three support structure concepts are developed for a newly-designed two-bladed downwind 14 MW wind turbine, named 2B14. A finite-element (FE) model for all three concepts is developed, consisting of a simplified rotor-nacelle assembly (RNA) model of the 2B14 and the corresponding support structure. The discretized stiffness and mass assembly is then used as input for fully-coupled aero-hydro-servo-elastic simulations carried out by the software Bladed V4.6. The numerical model allows to quickly define the global dimensions for a given target natural frequency, satisfying a chosen ultimate limit state (ULS) criterion. The three concepts are first compared in terms of estimated mass. Afterwards, an iterative modal analysis is carried out in order to assess the dynamic interaction between the two-bladed rotor and the support structure. In such regard, peculiar dynamic phenomena such as veering [8], mode hybridization and mode coalescence [9] are observed, in particular for the two space-frame structures. Given the significant difference in terms of dimensions between a monopile and the structural parts of a space-frame concept, the resulting hydrodynamic loads are quantified and the sensitivity of the dynamic behaviour due to variations of the soil flexibility is highlighted.

2. Description of the three design concepts

2.1. Wind turbine description

The 2B14 wind turbine used in this work is a result of a research project which involves several industrial partners and Delft University of Technology. One of the main project goals consists in the development of a next generation 12–15 MW offshore wind turbine concept. The 2B14 is a 14 MW two-bladed wind turbine which operates in a downwind configuration, designed within the wind class IEC1B. The turbine relies on a variable speed, pitch-regulated controller which operates on each blade individually in order to reduce the nodding loads. Differently from a three-bladed rotor, the 2B14 induces a nodding and a yaw moment of inertia which depend on the azimuth position of the rotor. Both moments of inertia vary of an order of magnitude with a 90° change of the azimuth angle. The main parameters characterizing the RNA are the speed range of the rotor (3.0–8.4 rpm), the rotor diameter (220.6 m) and the mass (926 tonnes).

A two-bladed downwind configuration has a better yaw stability compared to an upwind configuration [10]. Furthermore, the downwind setup reduces the risk of the blades to hit the supporting structure, therefore there is no need of blade pre-bending [11]. This opens up the opportunity to develop and install more flexible and softer blades with a consequent reduction of the blade fatigue loading [12, 13].

2.2. Design procedure

A fair comparison between the three design concepts requires some shared design constraints that need to be fixed in advance. The first constraint is given by a single target natural frequency for all three support structures in order to avoid possible resonance phenomena with the operational and environmental dynamic loading. The operational dynamic load refers to the rotor frequency, while the wave regime is described by the JONSWAP spectrum. Figure 1a represents the operational frequencies through a Campbell diagram, including the assumed wave regime. The thin green patch in Fig. 1a highlights the selected dynamic design range which should allow a relatively flexible support structure. For design simplicity, the second constraint implies to use

the same upper tower for the monopile and the jacket support structure and the same space-frame configuration for the jacket support structure and the lattice tower. The third constraint refers to the design levels such as seabed level, interface level and hub height which are kept constant. Scour protection and a water depth of 50 m are assumed. The last constraint involves the connections. The tubular elements of the lattice tower are connected through welded joints. A grouted connection is used between the transition piece and the monopile foundation, while a welded connection is assumed between the transition piece and the jacket support structure.

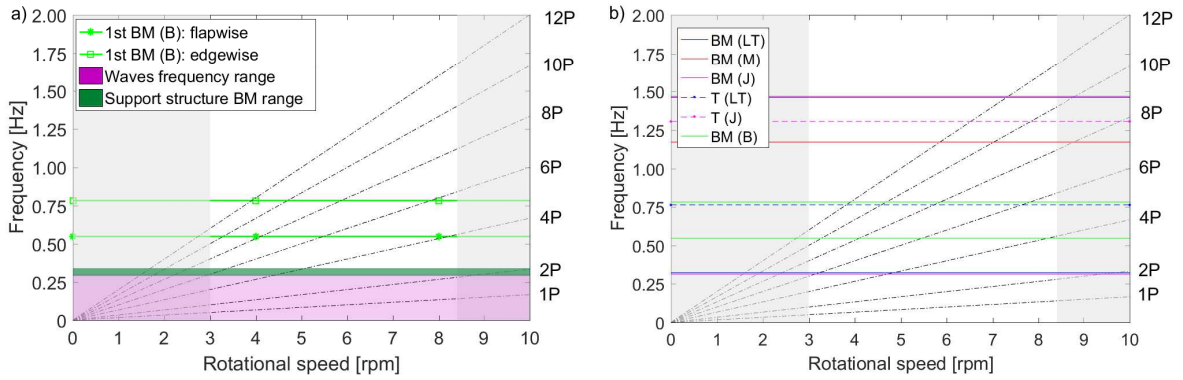

Figure 1: a) Campbell diagram, wave frequency range and desirable natural frequency range of the support structures for the 2B14 turbine. The white area delimitates the operational range; b) estimated natural frequencies of the three design concepts. BM and T stand for bending mode and torsional mode, respectively. LT, M and J refer to lattice tower, monopile and jacket structure, whereas BM (B) indicates the blade bending modes.

Based on the chosen constraints, the design procedure for all three concepts runs through four different steps. During the first step, the interface level is obtained based on the extreme water level variation and wave conditions presented in the UpWind report [14]. The hub height is then inferred from the estimated interface level, taking into account the turbine rotor size and the blade clearance. The second step estimates the initial dimensions for all three concepts by imposing the target design natural frequency shown in Fig. 1a and a fixity depth for the foundation piles. The third design step relaxes the assumption of the fixity depth introducing soil mechanics effects by means of distributed lateral and axial linear springs along the foundation piles. The stiffness values of the soil springs were retrieved from a more detailed soil-structure interaction analysis carried out with OpenSeesPL, where different soil layers were introduced based on the site description provided by the UpWind report [14]. This approach has been preferred to the P-Y curves, since the latter approach requires a FE model validation for diameters higher than 1 m. Given the identified stiffness values and the chosen extreme environmental loads, the embedded length of the piles were estimated by imposing constraints on maximum deflections, rotations and bearing capacity. The last design step provides a comparison between the updated first natural frequencies and the target design frequencies (Fig. 1b). If the new natural frequencies fall outside the desirable design domain, the design procedure is repeated again starting from step two.

2.3. Schematic layout of the three design concepts

Figure 2 shows an assonometric view of the geometric model for each design concept. The jacket and the lattice tower consist of a four legged space-frame structure made out of tubular steel elements. In general, these type of structures are subject to lower wave loads compared to a

monopile support structure [15]. The legs and bracings are connected through welded K-joints, while bracings within the inclined plane between the legs have a welded X-joint configuration. Differently from the jacket structure, the lattice tower provides a direct support for the RNA without a transition to a tubular tower.

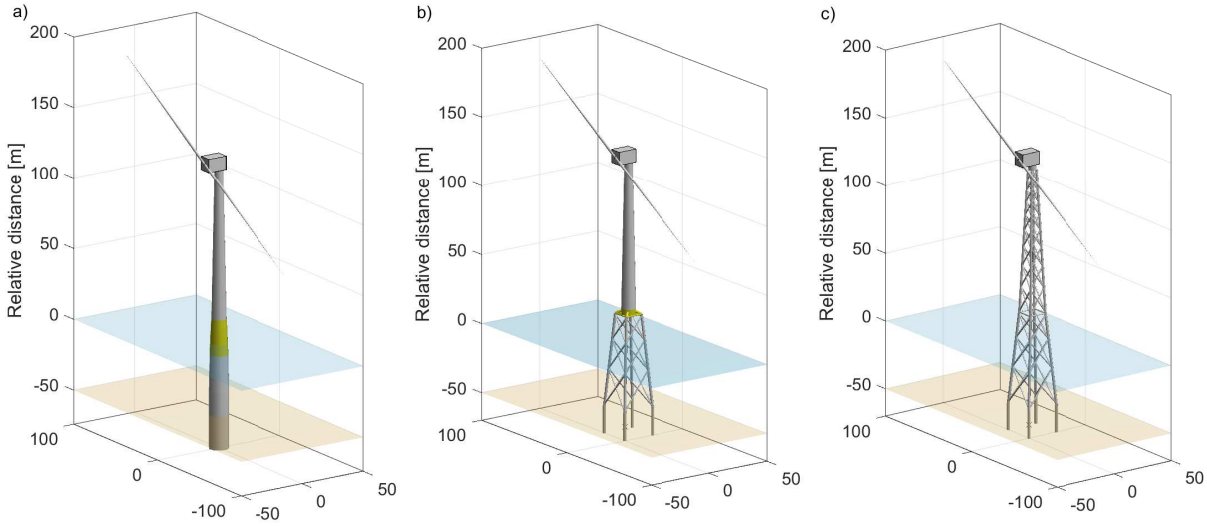

Figure 2: Assonometric view of the geometric model for each design concept: a) monopile; b) jacket structure; c) lattice tower.

3. FE model, ULS and design dimensions

3.1. Description of the FE modelling approach

The FE models for each design concept are developed by assembling Timoshenko beam elements. Each node of the beam element is characterized by six degrees of freedom (i.e. three translations and three rotations). The interaction between soil and foundation piles is modelled by means of linear spring elements. The RNA is modelled by taking into account its six inertial contributions which are placed at the centre of the RNA's mass. Note that the centre of mass is eccentric with respect to the vertical neutral axis of the support structure. The resulting rigid body of the RNA is then connected to the top of the corresponding support structure through a rigid and massless element. The welded connections for the jacket structure and the lattice tower are modelled by assuming a transfer of shear, normal stress and bending moment in each connection. On the other hand, the steel-grout-steel connection of the transition piece is represented by an equivalent section that homogeneized the mass and the stiffness properties of both materials. The developed FE models are then used to run static and modal analysis. In addition, the geometric and mechanical properties of the developed models can then be used as input data for a more detailed servo-aero-hydro-elastic simulations carried out in Bladed V4.6.

3.2. ULS yield check and main design dimensions

The stress analysis is performed by assuming a normal safety factor on the applied loads and on the material strength according to [16]. The applied loads are simulated by selecting the DLC1.1 wind and wave loading conditions (see [16]). Regarding the wind load, a normal turbulence model was assumed with a mean wind speed at hub height equal to 11 m/s and a turbulence intensity of 14%. Irregular waves are assumed with a significant wave height of 7.1 m and a peak period of 9.4 s. The wave loads are modelled by Morison's equation, including a diffraction correction.

For the simulations, two different wind directions are assumed, 0° and 45° with respect the north orientation of the support structure. For each wind direction, three different wind–wave misalignments were considered, 0°, 45° and 90°.

After comparing the simulated results, a ULS yield check [17] is carried out by assessing the material utilization factor that relates the highest normal stress (tensile or compressive) in a specific cross-section to the material yield strength. The normal stress refers to in-plane and out-of-plane bending moments combined with the normal force acting in the corresponding structural element. Torsion- and shear-induced stress were neglected. Figure 3 shows the yield check results for each design concepts, highlighting the structural element with the highest estimated normal stress. The material utilization factors of all concepts are fairly comparable.

In terms of final dimensions, the hub height is assumed to be equal (132.65 m) for all three design concepts. For the sake of synthesis, only the dimensions of the substructures are provided. The bottom and top diameters of the monopile are 11.1 m and 14 m, respectively, the length is equal to 93 m and the wall thickness changes from 140 mm to 93 mm. In relation to the space-frame structures, the base and top widths are 24 m and 13 m, respectively, whereas the height is 67.15 m. The diameter of the legs is 2 m with a wall thickness equal to 50 mm.

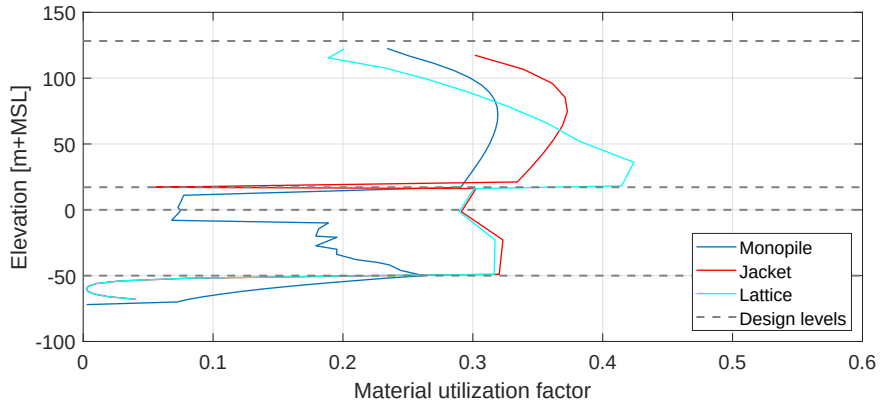

Figure 3: Material utilization factor for the most stressed structural element of each design concept.

4. Comparative analysis

4.1. Mass reduction

Table 1 summarizes the masses of the main structural parts for each design concept. For comparison, the total mass of the substructure M_{tot} is normalized to the RNA mass, M_{RNA}. The results show that the jacket and the lattice tower allow for a significant mass reduction. Both types of structure exhibit a M_{tot}-to-M_{RNA} ratio almost equal to 3, whereas the monopile approaches a value of 7. The estimated large mass for the monopile concept is needed in order to comply the target natural frequency shown in Fig.2 and the given constraints such as design levels and RNA mass. It is worth highlighting that the adopted design approach was rather simple. Possibly, a different design solution for the monopile can be sought that may allow keeping the stiffness to mass ratio constant, while reducing the mass of the substructure. On the other hand, note that the lattice tower design is based on keeping the respective cross-sections of the various structural elements constant, which is inefficient from a mass reduction perspective. However, whether an optimal design strategy is adopted or not, the mass difference between the lattice tower and the monopile would be still significant.

The most significant mass reduction refers to the foundation piles, for which the difference between the monopile and the two space-frame structures is of an order of magnitude. Note that

the mass provided for both space-frame structures refers to four slender piles. The substructure of the monopile turned out to be 1.5 times heavier than the substructure of both space-frame structures. Consider also that for the latter two structures the mass is slightly increased to account for the coating in the splashzone (see Fig.2), while for the monopile the coating is included in the transition piece.

A comment apart is needed for the transition piece of the monopile which accounts for a total mass of 1300 tonnes, including the grout mass (374 tonnes). The latter mass could be significantly reduced if a different solution to connect the tower and the monopile is adopted. For example, a slip-joint solution [18] may reduce the mass up to 400 tonnes, while a bolted connection may almost get rid of most of the transition piece mass.

Table 1: Mass values of the different structural parts for each design concept.

Structural parts	Monopile	Jacket	Lattice tower
Foundation piles [tonnes]	1149	103	103
Substructure [tonnes]	2526	1058	1090
Transition piece [tonnes]	1300	278	n.a.
Tower [tonnes]	1251	1252	1314
Total mass M [tonnes]	6171	2692	2506
$M_{\mathrm{tot}}/M_{\mathrm{RNA}}$ [-]	6.67	2.91	2.71

The mass has a direct link to the construction cost of each design concept. Even though a detailed economical comparison falls outside the scope of this work, it is worth introducing a qualitative discussion on possible costs for each design concept. For example, the manufacturing between the different design concepts may differ significantly. Steel tubular structures used for monopiles are typically more cost-efficient than structural elements used for a space-frame concept [19]. However, the technology for automated manufacture of space-frame structures is inevitably advancing, cutting costs and concurrently improving the weld quality. The tubular monopile structure also provides a protected space for equipment and access for personnel, while the lattice tower would require secondary steel structures and therefore additional costs.

4.2. Interaction between structural dynamics and excitation frequency

As mentioned above, the adopted two-bladed wind turbine induces a yawing and nodding moment of inertia that are both varying quantities depending on the rotor's azimuth position. In general, the dynamics of all three support structures are affected by these time-varying inertial terms [20]. Specifically, both space-frame structures show the most significant influence resulting in veering, mode coalescence and mode shape hybridization phenomena [8, 9]. In order to highlight the aforementioned dynamic effects, the dynamic behaviour of the lattice tower is taken as an illustrative example. It is worth mentioning that the jacket-based design concept exhibited the most complex behaviour, which certainly calls for future investigation.

Figure 4 shows the variation of the first five natural frequencies caused by a change of the rotor's azimuth angle. It can be observed that all frequencies tend to "cross" each other. Note that the crossing is only an apparent phenomenon since the structure is not entirely symmetric. Therefore, the modes are not fully uncoupled [8]. In fact, the induced eccentricity of the RNA with respect to the vertical axis of the support structure provides a slight coupling among the modes, causing the natural frequencies to veer rather than to cross. The first and second bending mode shapes switch position between the fore-aft and side-side directions at an azimuth angle

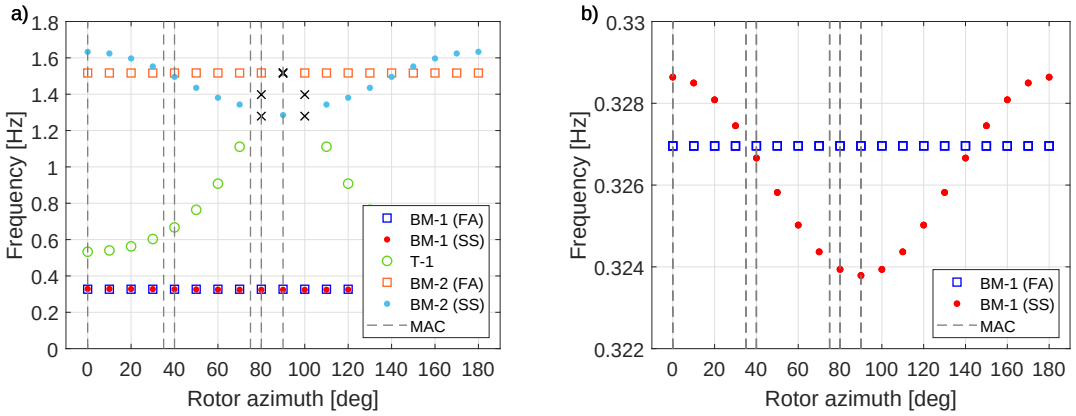

Figure 4: a) Variation of the first five natural frequencies of the lattice tower with respect to the rotor's azimuth; b) variation of the first two bending modes. BM and T refer to the bending and torsional modes, respectively. FA and SS indicate the fore–aft and side–side directions. The grey dashed lines define the angles for which the MAC index was computed.

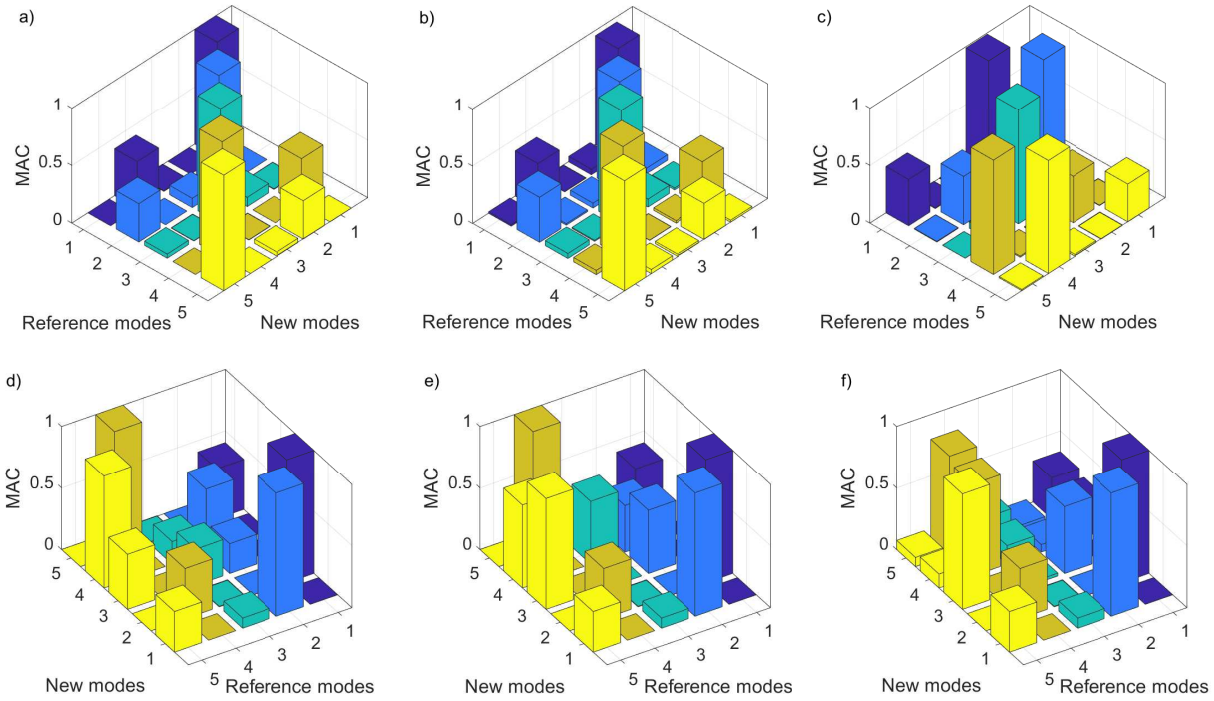

Figure 5: Variation of the first five mode shapes with reference to an azimuth angle of 0°. The variation is assessed by means of the MAC index: a) 0°; b) 35°; c) 40°; d) 75°; e) 80°; f) 90°.

next to 40°. A similar behaviour was also found for the first bending modes of a monopile supporting a lab-scale two-bladed wind turbine [20]. Note that the switch of the second bending mode shapes is more evident compared to the first bending mode shapes.

The effect induced by the dynamic interaction between the rotor and the support structure is clearly visible by inspecting the variation of the torsional mode in Fig. 4a. Within a narrow angle range, between 75–90°, the torsion mode switches between the third and the fourth position.

Eventually, at an angle of 90°, the torsional mode tends to merge with the side-side second bending mode, almost resembling a mode coalescence phenomenon [9]. It is worth highlighting that in the aforementioned narrow azimuth angle range, the mode shapes of the last three natural frequencies cannot be straightforwardly classified as bending or torsion due to the hybridization between the modes caused by the veering phenomenon. The black crosses in Fig. 4a point out the aforementioned hybridized modes.

In order to assess the variation and the hybridization of the first five mode shapes, the modal assurance criterion (MAC) is used as a correlation index [21]. The MAC index quantifies the consistency between the first five mode shapes estimated at a specific azimuth angle and the reference modes computed at an azimuth of 0°. Figure 5 provides an informative summary of the MAC values estimated at chosen azimuth angles. The index is bounded between 0 and 1, were 1 indicates a complete consistency between the mode shapes. Figure 5b is almost identical to the reference case in Fig. 5a, apart from a imperceptible increase of coupling between the FA and SS bending modes. The complete switch between the FA and SS bending mode is clearly visible in Fig. 5c. The last three MAC plots, Figs. 5d–f, highlight a more mixed up consistency among the mode shapes for which a clear classification of bending and torsion is not possible anymore. In order to visualize the hybridization of the torsional mode, the corresponding modal shape is plotted in Fig. 6 for an azimuth angle of 40°, 75° and 80°. Both mode shapes in Figs. 6b–c clearly show the hybridization and coupling between a bending and torsional behaviour.

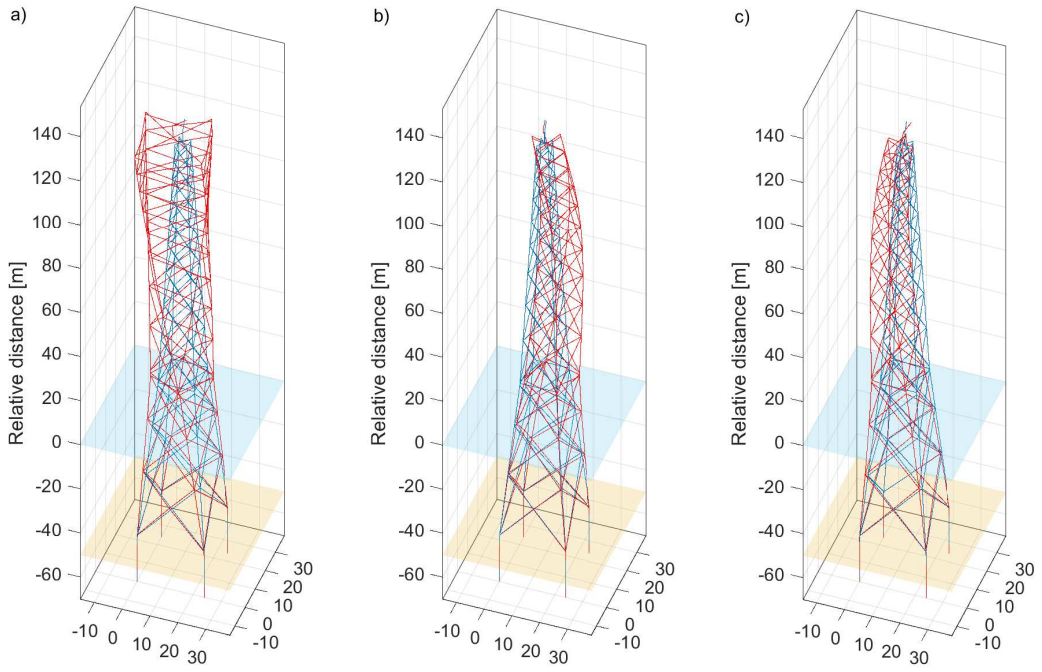

Figure 6: Snapshots of the torsional mode shapes for an azimuth angle of: a) 40°; b) 75°; c) 80°.

4.3. Hydrodynamic loads and soil-structure interaction

In general, a monopile support structure can be subject to higher hydrodynamic loads than a space-frame one. To preliminarily assess this difference, a DLC6.1 hydrodynamic loading according to [16] was adopted. The sea state is characterized by a significant wave height of 9.4 m and a peak period of 13.7 s. Table 2 and 3 present the resulting hydrodynamic force and the mudline bending moment as well as the standard deviation σ, respectively, for both the

monopile and the space-frame support structures. It can be seen that the total hydrodynamic force on the monopile foundation is more than six times larger than the force on the space-frame structures, whereas the standard deviation is more than 16 times larger. Regarding the mudline moment, the maximum value is more than three times larger for the monopile and the standard deviation is more than five times larger. For the space-frame structures it was observed that the wave directionality is a negligible parameter.

Table 2: Hydrodynamic force.

	Max. [MN]	σ [MN]
Monopile	20.43	5.89
Space-frame	3.23	0.35

Table 3: Mudline moment.

	Max. [MNm]	σ [MNm]
Monopile	629.6	183.0
Space-frame	192.2	33.82

The sensitivity of the dynamic behaviour of the three design concepts towards the soil-structure interaction is shown in Fig. 7 for which medium dense sand was assumed. Fig. 7a assesses the relevance of the vertical and lateral soil flexibility, where the blue coloured points are obtained by assuming the soil to be laterally rigid and flexible in the vertical direction, whereas for the red coloured point the opposite assumption was made. The highest frequency variation was observed for the monopile concept, which exhibits a significant sensitivity with respect to the lateral soil flexibility. The overall sensitivity of the space-frame structures is smaller compared to the monopile. Contrarily to the monopile, the space-frame concepts show a higher sensitivity towards the axial flexibility of the soil. In Fig. 7b the sensitivity ratios (SR) for each design concept are presented. In general, the SRs highlight a nonlinear relation between natural frequency and the chosen soil type. Specifically, the most significant sensitivity is observed for the monopile.

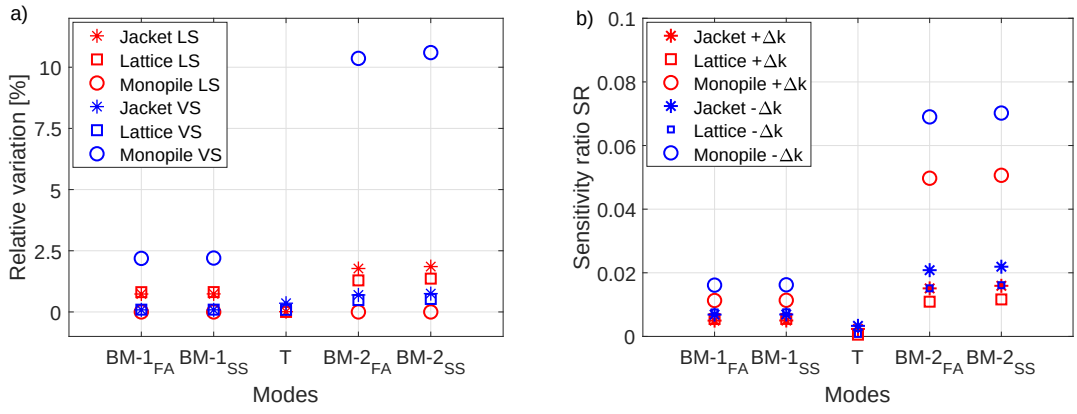

Figure 7: a) Relevance of vertical (VS) and lateral (LS) soil flexibility; b) Sensitivity ratio SR, where SR $= \frac{\Delta f}{\Delta k}\frac{f_{ref}}{k_{ref}}$. The variation Δk is assumed to be 20% of the reference stiffness k_{ref}, whereas Δf is the frequency variation with respect to the reference frequency f_{ref}.

5. Conclusions

The comparative analysis of the three design concepts shows that for the space-frame structures a significant reduction of the total mass can be achieved during a preliminary design stage. With regard to the dynamic behaviour, the analysis of the time-varying modal characteristics of the three concepts shows a strong influence of the RNA's yaw moment of inertia on the

first set of natural frequencies. This is relevant especially for both space-frame structures, for which dynamic phenomena such as veering, mode coalescence and mode shape hybridization were observed. In particular, the torsional mode of both structures seemed to be mostly affected by all three aforementioned behaviours. Note that these phenomena are strictly linked to the assumed coupling between the RNA and the support structure. In the case of a passive yaw system, the aforementioned dynamic effects can be mitigated by introducing a torsional decoupling between the RNA and the support structure. In terms of soil-structure interaction, both space-frame structures showed a lower sensitivity to the uncertainty of the soil flexibility compared to the monopile concept. At last, the hydrodynamic load analysis highlighted that the monopile is subject to the highest hydrodynamic force. Based on these preliminary results, the full-height lattice structure seems to exhibit the highest potential to support large wind turbines in deep water sites. For a more fair cost assessment for each design concept, a future and more detailed comparison should extend the ULS structural analysis, including buckling and fatigue failure.

Acknowledgement
The 2B1X project is funded by Netherlands Enterprise Agency. The authors would like to acknowledge all the industrial partners of the project, 2-B Energy Holding BV, TRES4 BV and Bayards Aluminium Constructions BV, for providing the necessary data to carry out the comparative analysis and for their comments and feedback on the manuscript.

References

[1] Leimester M and Dose B 2018 Validation and Development of Improved Methods for the Calculation of Wave Loads on XXL Monopiles *Proc. of Int. Conf. on Ocean, Offshore and Arctic Engineering*, Madrid, Spain, June 17-22
[2] Ahmed S S and Hawlader B 2016 Numerical analysis of large-diameter monopiles in dense sand supporting offshore wind turbines *Int. J. Geomech.* **16**(5) 04016018
[3] Damgaard M, Bayat M, Andersen L V and Ibsen L B 2014 Assessment of the dynamic behaviour of saturated soil subjected to cyclic loading from offshore monopile wind turbine foundations *Comput. Geotech.* **61** 116-26
[4] Damiani R, Dykes K and Scott G 2016 A comparison study of offshore wind support structures with monopiles and jackets for U.S. waters *J. Phys.: Conf. Ser.* **753** 092003
[5] Farhan M, Reza M, Mohammadi S, Correia J A and Rebelo C 2018 Transition piece design for an onshore hybrid wind turbine with multiaxial fatigue life estimation *Wind Engineering* **42**(4) 286-303
[6] Muskulus A 2012 The Full-height Lattice Tower Concept *Enrgy Proced.* **24** 371-77
[7] Natarajan A, Stolpe M and Wandji W N 2019 Structural optimization based design of jacket type sub-structures for 10MW offshore wind turbines *Ocean Eng.* **172** 629-40
[8] Balmès E 1993 High modal density, curve veering, localization: a different perspective on the structural response *J. Sound Vib.* **161**(2) 358-63
[9] Triantafyllou M S and Triantafyllou G S 1991 Frequency coalescence and mode localization phenomena: A geometric theory *J. Sound Vib.* **150**(3) 485-500
[10] Kress C, Chokani R and Abhari S 2015 Downwind wind turbine yaw stability and performance *Renew. Energ.* **83** 1157-65
[11] Koh J H and Ng E Y K 2016 Downwind offshore wind turbines: Opportunities, trends and technical challenges *Renew. Sust. Energ. Rev.* **54** 797-808
[12] Reiso M and Muskulus M 2013 The simultaneous effect of a fairing tower and increased blade flexibility on a downwind mounted rotor *J. Renew. Sustain. Ener.* **5** 033106
[13] Reiso M, Hagen T R and Muskulus M 2013 A calibration method for downwind wake models accounting for the unsteady behaviour of the wind turbine tower shadow behind monopile and truss towers *J. Wind Eng. Ind. Aerod.* **121** 29-38
[14] De Vries W, Vemula N K, Passon P, Fischer T, Kaufer D, Matha D, Schmidt B and Vorpahl F 2011 *Final report WP 4.2: Support Structure Concepts for Deep Water Sites*
[15] Shi W, Park H-C, Chung C and Kim Y-C 2011 Comparison of dynamic response of monopile, tripod and jacket foundation system for a 5-MW wind turbine *Proc. of the Int. Offshore and Polar Engineering Conf. ISOPE*, Maui, Hawaii, USA, June 19-24, 263-69
[16] DNV-GL, 2016 *Loads and site conditions for wind turbines*, DNVGL-ST-0437

[17] DNV-GL, 2014 *Design of offshore wind turbine structures*, DNVGL-OS-J101
[18] Cabboi A, Segeren M, Hendrikse H and Metrikine A 2020 Vibration-assisted installation and decommissioning of a slip-joint *Eng. Struct.* **209** 109949
[19] Wagner H J, Matur J 2012 *Introduction to Wind Energy Systems: Basics, Technology and Operation* (Berlin: Springer)
[20] Larsen T J and Kim T 2015 Experimental and Numerical Study of a New Dynamic Phenomenon for Two-bladed Wind Turbines *Proc. of the Int. Offshore and Polar Engineering Conf. ISOPE*, Kona, Hawaii, USA, June 21-26, 547-53
[21] Ewins D J 2012 *Modal testing: theory, practice, and application* (Baldock Hertfordshire: Wiley)